Whitmarsh, R.B., Sawyer, D.S., Klaus, A., and Masson, D.G. (Eds.), 1996
Proceedings of the Ocean Drilling Program, Scientific Results, Vol. 149

29. GEOCHEMISTRY OF WEATHERED MID-OCEAN RIDGE BASALT AND DIABASE CLASTS FROM HOLE 899B IN THE IBERIA ABYSSAL PLAIN[1]

Karl Seifert[2] and Dale Brunotte[2]

ABSTRACT

Ocean Drilling Program Hole 899B on the Iberia Abyssal Plain penetrated a thick serpentinite breccia flow underlain by smaller breccia flows, all separated by sediments containing weathered basalt and diabase (microgabbro) clasts. The basalt and diabase clasts, some with discolored weathering rinds, recovered with Early Cretaceous sediments below the thick upper serpentinite breccia, have the compositional characteristics of mid-ocean ridge basalt (MORB) modified by weathering on the seafloor. Seafloor weathering has added MgO and K_2O and removed CaO from the clasts, resulting in strongly modified major element compositions. However, the more immobile trace elements remain largely unaltered, and all basalt and diabase clasts have rare-earth element and spidergram patterns similar to transitional to enriched MORB (E-MORB). The E-MORB clasts are similar to the type of mid-ocean ridge volcanism that later produced the Atlantic Ocean floor in the region of the present Azores Plateau. The incompatible element enrichment necessary to produce E-MORB indicates a plume contribution and suggests that Early Cretaceous rifting on the Iberia Abyssal Plain was plume initiated despite the lack of extensive volcanism.

INTRODUCTION

Leg 149 explored the ocean/continent transition (OCT) on the Iberia Abyssal Plain and its role in the opening of the Atlantic Ocean approximately 130 Ma. Leg 149 was the first of several legs in the Atlantic Ocean to study rifted-margin formation and evolution. Transects were chosen across both volcanic and nonvolcanic conjugate rifted margins with basement being the major drilling target. The Iberia Abyssal Plain was chosen as the best defined nonvolcanic rifted margin on the eastern edge of the Atlantic Ocean (Fig. 1); the geologically conjugate Newfoundland Margin was planned to be drilled on a later leg. The Iberia continental margin consists of several topographically distinct regions. In the northern part of the margin continental crust extends seaward under shallow water as the 200-km by 150-km Galicia Bank. The Galicia Bank contains a series of isolated seamounts along its southern edge and is separated from Iberia by a broad submarine valley. The Iberia Abyssal Plain lies south of the Galicia Bank (Fig. 2). Here the continental margin has a straight narrow shelf and a steep continental slope. South of 40°N the slope is cut by numerous deep canyons and at 39°N the east-west Estremadura Spur separates the Iberia Abyssal Plain from the Tagus Abyssal Plain that forms the southern part of the Iberia continental margin. South of the Tagus Abyssal Plain, the east-northeast Gorringe Bank marks the seismically active plate boundary between Eurasia and Africa.

Three main episodes of Mesozoic rifting marked the separation of the Iberia margin from the Newfoundland Grand Banks. The first episode was a Triassic to Early Jurassic rifting phase that produced graben and half-graben structures in which evaporites were deposited (Wilson et al., 1989; Murillas et al., 1990). A second rifting event consisted of extension in the Late Jurassic. A third episode of Early Cretaceous extension marked the south-to-north breakup of Iberia from the Grand Banks (Boillot, Winterer, Meyer, et al., 1987; Whitmarsh et al., 1990; Pinheiro et al., 1992). Only minor volcanism accompanied rifting, the crust is only 2-4 km thick, and the region contains no obvious seaward-dipping reflectors or subcrustal underplating. Plate reconstructions of Iberia with Europe and North America are difficult because Iberia was alternately attached to Europe and Africa (Srivastava et al., 1990).

Leg 149 was designed, on the basis of geophysical data, to drill across the entire OCT from the oceanic to the continental edge of the Iberia rifted margin but instead found an ocean-continent gap at least 130 km wide. The major drill targets on the Iberia Abyssal Plain were a series of basement highs (Fig. 3) beneath several hundred meters of sediment cover. The only basalt recovered on this leg occurred as weathered clasts associated with Early Cretaceous sediments below a thick serpentinite breccia flow at Hole 899B at a depth near 475 meters below the seafloor. The basalt and associated diabase clasts, referred to as microgabbro clasts in the *Initial Reports* volume (Sawyer, Whitmarsh, Klaus, et al., 1994), consequently could have either an oceanic or continental affinity. This geochemical study is designed to constrain the origin of the basalt and diabase clasts by determining the major and trace element compositions of whole rock samples and mineral compositions of phenocryst phases.

ANALYTICAL TECHNIQUES

A variety of analytical techniques are used because each technique determines certain elements better than others, and by combining techniques we obtain an accurate analysis of many elements. Major elements Si, Ti, Al, Fe, Mn, Mg, Ca, Na, K, and P were determined by inductively-coupled plasma (ICP) techniques, the oxidation state of Fe requires a separate titration, and H_2O^+, H_2O^- and CO_2 have been lumped into loss on ignition (LOI). Trace elements Ba, V, Cr, Ni, Zn, Cu, Pb, and Sr were also determined by ICP analysis. Fourteen rare earth elements (REEs), Sr, Ba, Th, Rb, Nb, Y, Hf, Ta, U, Pb, and Cs were determined by inductively-coupled plasma mass spectrometry (ICP/MS). All of the analyses were contracted out, except for the ferrous iron titrations, which were done at Iowa State University. ICP analyses were obtained from commercial laboratories (Chemex and Acme) and ICP/MS analyses were obtained from the GeoAnalytical Laboratory at Washington State University, Charles Knaack was the ICP/MS analyst. Accuracy of the ICP analyses was checked by including USGS standards BCR-1, BHVO-1

[1]Whitmarsh, R.B., Sawyer, D.S., Klaus, A., and Masson, D.G. (Eds.), 1996. *Proc. ODP, Sci. Results,* 149: College Station, TX (Ocean Drilling Program).

[2]Department of Geological & Atmospheric Sciences, Iowa State University, Ames, IA 50011, U.S.A. Seifert: kseifert@iastate.edu

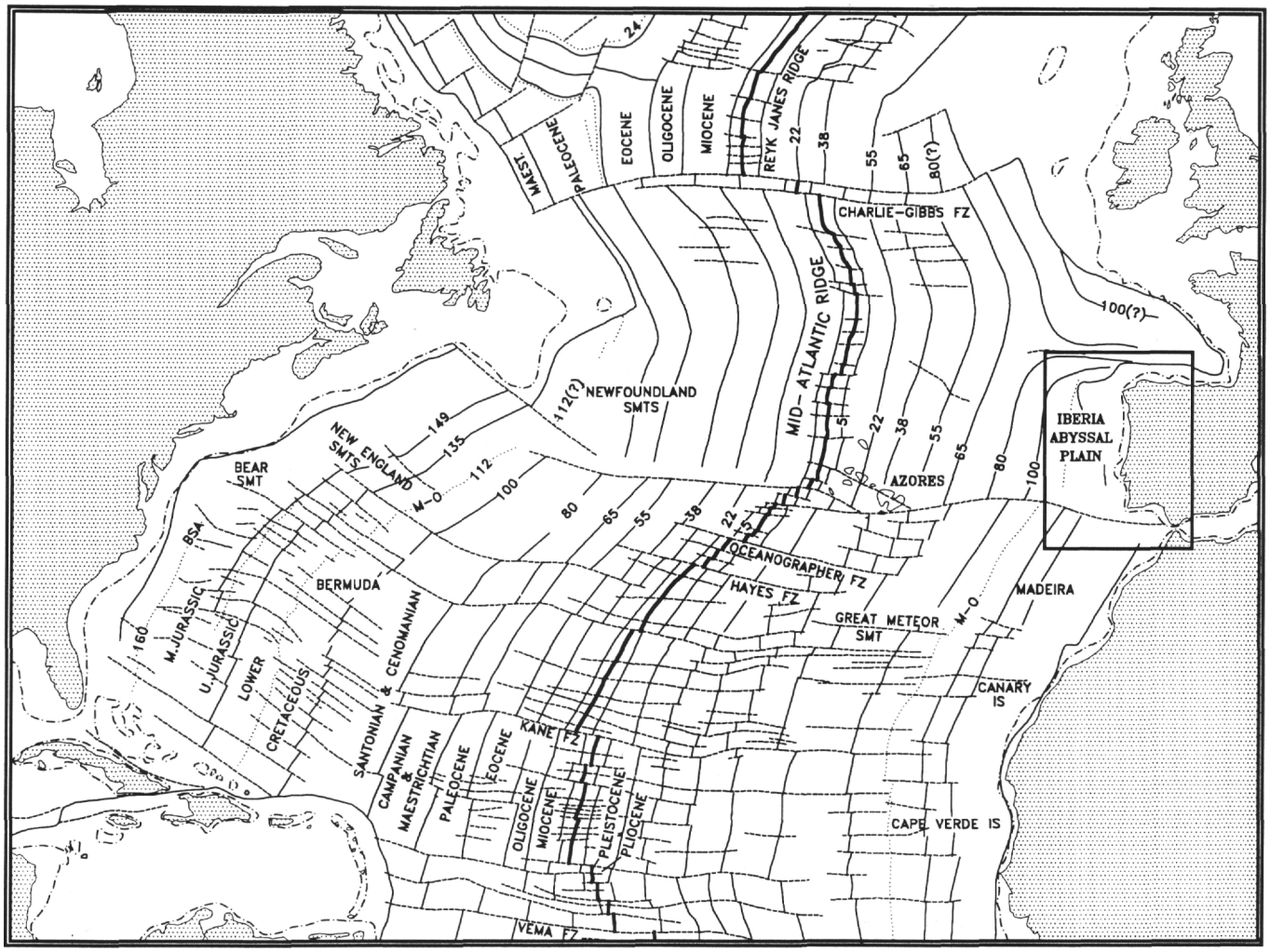

Figure 1. Map of the Atlantic Ocean showing the location of the Iberia Abyssal Plain and the geologically opposite Newfoundland Margin. Modified from Vogt and Perry (1981).

and NBS flyash 1633a as unknowns among the samples and repeated runs of the commercial laboratory in-house standards. Accuracy of the ICP/MS analyses was checked by a well-characterized BCR-1 clone from the same quarry (BCR-P) and other in-house standards used at the Washington State GeoAnalytical Laboratory. Precision of both the ICP and ICP/MS analyses was estimated at 5% to 10% from duplicate runs of standards and several unknowns, except near the detection limit which was 0.1 to 0.5 chondrite for trace elements run by ICP/MS. Trace elements run by both ICP and ICP/MS appear to have been more accurately determined by ICP/MS analysis and the ICP/MS data are preferentially reported in Table 1. Mineral compositions were determined with the Iowa State University electron microprobe using well-analyzed mineral standards obtained from various sources.

DESCRIPTION OF THE BASALT AND DIABASE CLASTS

Petrology

The pebble- to cobble-sized basalt clasts found in Early Cretaceous (Barremian- to early Aptian-aged) claystone and calcareous claystone below the thick breccia unit in Hole 899B exhibit a range of textures and vesicularity. Some basalt clasts are vesicular, and the vesicles are often filled with secondary white or pink minerals. Some basalt clasts have obvious discolored weathering rinds. Part of a highly altered autobrecciated basalt clast (interval 149-899B-26R-1, 115-118 cm) was analyzed in this study but no thin section was made because this friable rock fragmented badly during transport. The diabase clasts were called microgabbro clasts in the *Initial Reports* volume (Sawyer, Whitmarsh, Klaus, et al., 1994) because of a lack of obvious plagioclase laths regarded as characteristic of a diabasic texture. However, the diabase clasts have relatively short plagioclase laths and intergranular textures when observed in thin section and should be called diabase clasts rather than microgabbro clasts. Only ten nonvesicular and nonbrecciated basalt and diabase clasts were sampled for analysis and only eight of the ten clasts were thin sectioned. The five basalt clasts that were thin sectioned exhibit three distinctive textures that indicate different cooling histories and suggest derivation from separate sources, whereas the three diabase clasts have similar textures.

Two of the five thin-sectioned basalt clasts (interval 149-899B-27R-1, 19-26 cm, and interval 149-899B-29R-1, 99-102 cm) are porphyries in which 20% to 25% of the clasts consist of a range of large to small, twinned plagioclase phenocrysts with occasional zoning (Fig. 4). A microprobe traverse across one of the phenocrysts in a basalt clast from interval 149-899B-27R-1, 19-26 cm, indicates it has a relatively uniform composition near An_{80} (Fig. 5) and a low K content ($An_{80.76}$, $Ab_{19.07}$, $Or_{0.17}$). The plagioclase phenocrysts are relatively fresh in the basalt clast from interval 149-899B-27R-1, 19-26 cm, but are more badly altered in the basalt clast from interval 149-

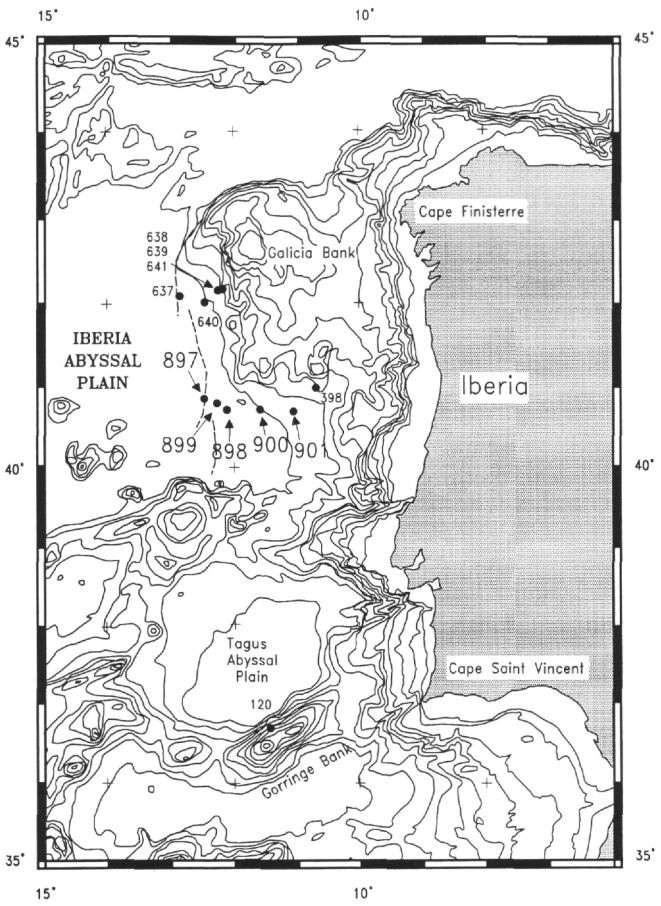

Figure 2. A map of the Iberia continental margin showing the location of the Leg 149 traverse and drill sites on the Iberia Abyssal Plain. Previous drill sites are also marked. The peridotite ridge drilled at Site 897, and on a previous leg at Site 637, is marked by a dashed line. Modified from Sawyer, Whitmarsh, Klaus, et al. (1994).

899B-29R-1,99-102 cm. What appear to be completely replaced olivine phenocrysts also occur in both of these porphyries. Two other basalt clasts (interval 149-899B-27R-1, 13-15 cm, and interval 149-899B-31R-1, 9-14 cm) have spherulitic to variolitic textures and the *Initial Reports* volume (Sawyer, Whitmarsh, Klaus, et al., 1994) refers to their variolitic texture. The remaining four clasts, a basalt clast from interval 149-899B-27R-1, 33-40 cm, and three diabase clasts from interval 149-899B-34R-1, 58-62 cm, interval 149-899B-35R-1, 0-7 cm, and interval 149-899B-36W-1, 37-42 cm, all have intergranular textures. Interval 149-899B-27R-1, 33-40 cm, contains a fine grained intergranular textured basalt that is badly altered with silicification and oxidation obscuring much of the original mineralogy. The other three intergranular textured clasts are coarser grained diabases that were called microgabbro clasts in the *Initial Reports* volume (Sawyer, Whitmarsh, Klaus, et al., 1994). These diabase clasts consist of 50% to 60% short plagioclase laths surrounded largely by fragments of clinopyroxene in various stages of alteration. The alteration material includes acicular masses of actinolite, brown biotite, and locally abundant iron oxide stain. The coarser diabase clasts must be derived from a flow interior, a dike, or a sill. The variable textures of the basalt clasts suggest a variety of sources rather than a single source. By contrast, the diabase clasts appear more uniform suggesting a single source. The source or sources of these clasts will be explored by comparing compositional data with that of typical basalts from known sources.

Major Element Geochemistry

The major element compositional variations observed in the basalt clasts indicate alteration by seafloor weathering. Several oxides vary systematically with changing LOI (Fig. 6) with most oxides decreasing with increasing LOI in what appears to be dilution caused by increasing LOI. However, MgO increases dramatically with increasing LOI while total iron increases slightly, suggesting addition of these components to the rock from the altering solutions. Also the CaO content decreases much more rapidly with increasing LOI than other oxides, suggesting a loss to the altering solutions. The most altered basalt clast (interval 149-899B-26R-1, 113-118 cm), in which LOI = 13.4%, has a much altered composition, with CaO = 0.76%, $A1_2O_3$ = 11.24%, and MgO = 28.66%, when calculated dry. This argues strongly for removal of CaO, addition of MgO, and perhaps some removal of $A1_2O_3$. The other basalt clasts, which have lower LOI values, but similar oxidation values, reveal more typical basalt compositions when calculated dry, except for CaO and MgO which are unusually low and unusually high, respectively, and show a strong negative correlation (Fig. 7). The influence of the added MgO can be observed on an alkali-iron-magnesium (AFM) diagram (Fig. 8), where the basalt clasts plot off the high MgO end of the Skaergaard magma evolution trend in a region where cumulates typically plot. Because MgO and FeO_t increase together in these altered clasts, the effect illustrates greater addition of MgO rather than depletion of FeO_t.

Experimental studies (Bischoff and Seyfried, 1978; Hajash, 1975; Humphris and Thompson, 1978; Mottl and Holland, 1978; Seyfried and Bischoff, 1979; Hajash and Archer, 1980) have determined that altered basalt gains Na and Mg from seawater and loses Ca, Fe, Mn, and Si to seawater at all experimental conditions. The relative extent to which various elements are exchanged between basalt and seawater depends primarily on temperature and the water/rock ratio (Hajash and Archer, 1980). Consequently, the increase in MgO and loss of CaO in basalt clasts occurs at all temperatures and water/rock ratios and provides no information on the conditions of alteration. However, the gain of K_2O by the basalt and diabase clasts indicates low temperature alteration, below 200°C (Seyfried and Bischoff, 1979), in agreement with observations of K_2O gains from seafloor weathering (Thompson, 1973, Thompson and Humphris, 1977). Above about 200°C, K_2O appears to be lost from basalt to seawater (Bischoff and Dickson, 1975; Mottl and Holland, 1978). The relative change in concentrations of other major elements due to seawater alteration is typically less clear.

Variations in major element composition not obviously related to seafloor weathering may reveal some indication of the petrogenesis of the six basalt clasts. Perhaps the most significant variation is shown by TiO_2 (0.64% to 1.84%), calculated dry, which does not correlate with variations in the degree of alteration as estimated from LOI content, LOI = 4.4% to 13.4%, and the oxidation ratio, Fe_2O_3/FeO = 0.37 to 1.10. The basalt clast from interval 149-899B-27R-1, 19-26 cm, has low TiO_2 (0.64%), and low K_2O (0.31%), compared to the other clasts which all have TiO_2, and K_2O, values over 1 %, suggesting a distinct source from the other basalt clasts. The low TiO_2 clast is also more depleted in incompatible trace elements such as Ba, Zr, and Sr.

Much of the major element compositional variation in the diabase (microgabbro) clasts is similar to that noted in the basalt clasts and can also be attributed to seafloor weathering. Several of the major element oxides decrease progressively with increasing LOI content (Fig. 9), in the manner observed for the basalt clasts, but with less scatter. The smaller degree of scatter in the diabase clasts relative to the basalt clasts could be because of a smaller sample set, or a smaller range of LOI variation, or it could be interpreted to suggest that the texturally similar diabase clasts started with a more similar major element composition and perhaps from a common source. Although

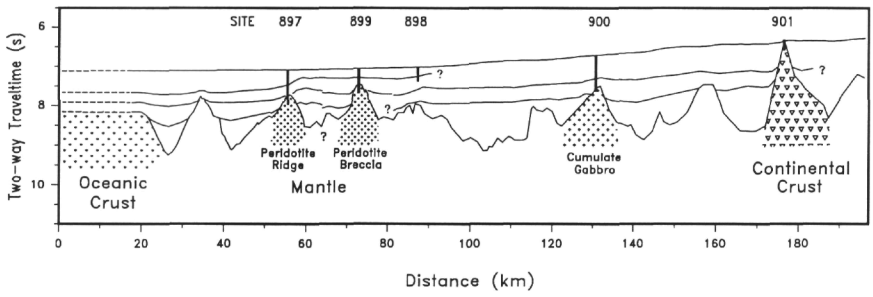

Figure 3. A roughly east-west geologic cross section across the Iberia Abyssal Plain showing the topography of the basement highs drilled on Leg 149 and located on Figure 2. Vertical exaggeration is 5×. Modified from Sawyer, Whitmarsh, Klaus, et al. (1994).

Table 1. Major and trace element composition of Hole 899B MORB and diabase clasts.

	Basalt clasts						Diabase clasts			
Core, section:	26R-1	27R-1	27R-1	27R-1	29R-1	31R-1	33R-1	34R-1	35R-1	36W-1
Interval (cm):	113–118	13–15	19–26	33–40	99–102	9–14	25–31	58–62	0–7	37–42
Major elements										
SiO_2	40.30	47.68	46.51	46.56	48.49	43.78	33.97	48.16	47.94	45.30
TiO_2	0.98	1.33	0.61	1.68	1.00	1.53	1.25	0.70	O.75	1.01
Al_2O_3	9.65	15.97	20.33	13.03	19.60	15.69	15.07	16.82	17.27	15.07
Cr_2O_3	0.01	0.04	0.03	0.01	0.04	0.03	0.03	0.03	0.04	0.03
Fe_2O_3	2.51	1.66	1.93	2.98	2.29	2.18	2.55	1.96	1.19	1.81
FeO	5.10	4.50	3.85	5.29	2.09	4.91	6.96	5.06	5.34	6.03
MnO	0.13	0.13	0.12	0.18	0.04	0.08	0.19	0.08	0.10	0.13
MgO	24.62	11.89	8.89	14.79	9.77	16.45	24.63	11.07	11.26	13.87
NiO	0.01	0.03	0.03	0.01	0.01	0.03	0.02	0.02	0.02	0.03
CaO	0.65	5.68	9.81	1.58	4.88	2.35	1.10	1.75	1.89	2.49
Na_2O	1.13	2.54	2.64	3.02	2.77	2.32	0.39	1.96	2.46	2.84
K_2O	0.67	1.99	0.29	1.73	1.91	1.21	0.31	4.67	3.95	1.72
P_2O_5	0.25	0.32	0.09	0.42	0.34	0.30	0.27	0.09	0.09	0.12
LOI	13.40	5.60	4.40	8.00	6.50	8.50	12.40	7.00	7.00	8.60
TOTAL	99.41	99.36	99.53	99.28	99.73	99.36	99.14	99.37	99.30	99.05
FeO_t	7.36	5.99	5.59	7.97	4.15	6.88	9.26	6.82	6.41	7.66
Fe_3/Fe_2	0.49	0.37	0.50	0.56	1.10	0.44	0.37	0.39	0.22	0.30
Mg#	88	81	77	80	83	83	85	77	79	79
Trace elements										
La	9.79	13.8	2.77	14.0	6.54	13.9	—	3.34	3.55	—
Ce	23.5	28.8	6.53	31.1	14.8	33.4	—	7.45	8.10	—
Pr	3.07	3.61	0.96	4.08	2.05	4.71	—	1.05	1.08	—
Nd	14.1	16.0	4.87	18.6	9.64	23.1	—	5.07	5.08	—
Sm	3.81	3.93	1.69	4.84	2.99	6.28	—	1.68	1.67	—
Eu	1.11	1.30	0.77	1.44	1.16	2.11	—	0.77	0.78	—
Gd	3.79	3.75	1.97	4.79	3.29	6.71	—	2.10	2.14	—
Tb	0.69	0.65	0.41	0.88	0.63	1.15	—	0.45	0.45	—
Dy	4.17	3.89	2.68	5.18	3.93	6.84	—	2.97	2.79	—
Ho	0.86	0.78	0.58	1.09	0.80	1.33	—	0.65	0.60	—
Er	2.41	2.13	1.63	3.08	2.18	3.45	—	1.86	1.76	—
Tm	0.33	0.29	0.23	0.42	0.30	0.45	—	0.27	0.25	—
Yb	1.98	1.77	1.45	2.51	1.76	2.60	—	1.70	1.56	—
Lu	0.31	0.26	0.23	0.39	0.26	0.39	—	0.26	0.25	—
Y	22.5	21.3	15.5	28.9	21.2	38.1	—	17.7	15.7	—
Th	0.77	1.41	0.2	1.46	0.56	1.0	—	0.37	0.4	—
Nb	13.9	29.0	3.21	23.9	8.72	19.7	—	3.55	3.68	—
Zr	79	99	40	125	63	103	98	50	46	47
Hf	2.24	2.54	0.98	3.38	1.54	2.59	—	1.24	1.18	—
Ta	0.96	2.29	0.23	1.87	0.66	1.5	—	0.24	0.26	—
U	0.21	0.85	0.06	2.16	0.55	0.35	—	0.12	0.15	—
Pb	1.44	1.91	0.53	1.81	1.81	3.18	—	2.56	4.79	—
Ba	64	331	43	257	185	255	51	230	433	1255
Sr	66	264	240	122	241	216	39	132	147	481
Rb	9.48	34.6	5.8	38.5	24.2	20.1	—	45.5	31.7	—
Cs	0.07	0.08	0.29	0.08	0.55	0.17	—	0.63	1.04	—
Cu	23	43	89	27	<10	46	41	27	55	57
Zn	35	50	46	65	77	61	62	61	45	79
Co	13	37	45	25	5	38	28	31	48	27
Sc	17	26	24	21	33	29	25	25	24	27

Note: Mg# based on FeO = .85 FeO_t; $Fe_3/Fe_2 = Fe_2O_3/FeO$.

CaO values are very low in the diabase clasts, they do not vary systematically with LOI as in the basalt clasts. Instead K_2O and FeO_t are found to vary systematically in the diabase clasts. Both MgO and FeO_t increase with increasing LOI, with MgO again increasing dramatically, suggesting addition by seafloor weathering. The less altered diabase clasts have unusually high but irregular K_2O (1.90% to 5.06%), calculated on an anhydrous basis, and unusually low CaO (1.90% to 2.75%). The addition of K_2O to the less altered diabase clasts is similar to, but more extreme than, the addition observed in the basalt clasts. However, the most altered diabase clast (interval 149-899B-33R-1, 25-31 cm) with LOI = 12.4%, and a highly altered composition with MgO = 28.43%, SiO_2 = 39.21%, calculated on an anhydrous basis, has a low K_2O value of only 0.36%. This clast also has apparent small increases in FeO_t, MnO, P_2O_5, a large increase in Zr and, more significantly, a low abundance of trace elements Ba and Sr which are typically companion travelers with K. Perhaps a second event removed these soluble cations.

Trace Element Geochemistry

Trace elements provide greater resolution for distinguishing between basalts from various provinces than major elements because of

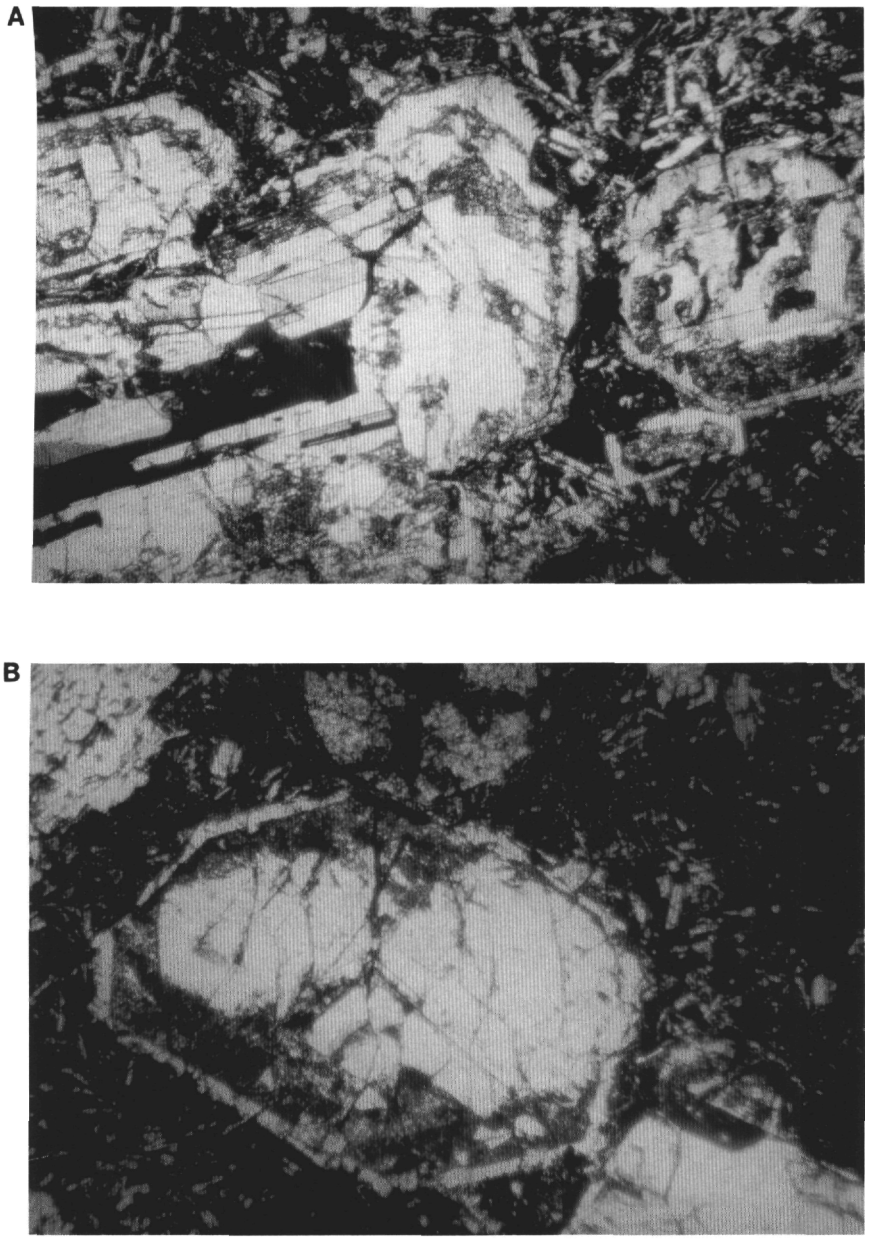

Figure 4. Photomicrographs of plagioclase phenocrysts from a basalt clast from interval 149-899B-27R-1, 19-26 cm, in cross polarized light (XLP). The long dimension of the photomicrographs is approximately 2.7 mm. Figure 4A shows a euhedral crystal outline and altered interior of a zoned plagioclase phenocryst. Figure 4B shows several plagioclase phenocrysts of varying size.

their greater variability. Because these basalt and diabase clasts occur in the transition zone between ocean and continent, they can have either a continental or oceanic source. Among the oceanic basalts, the mid-ocean ridge basalts (MORB) can be distinguished from ocean-island basalts (OIB) and island-arc basalts (IAB) by their elemental and isotopic concentrations. The ocean-plateau basalts (OPB) have elemental and isotopic characteristics that overlap with both MORB and OIB, but in most respects are more similar to MORB (Floyd, 1989; Castillo et al., 1991). However, no isotopic information has been obtained for these clasts, and comparisons must be based entirely on major and trace element compositions and compositional patterns. One of the more useful diagrams for identifying the source environment of basalts has been variably called a spider diagram, a spidergram, or an extended Corell-Masuda diagram because it involves several of the REEs. Sometimes the diagram is referred to as a spider diagram and the elemental data plot or plots on the diagram spidergrams. This usage will be followed here.

The sequence of major and trace elements used in spider diagrams reflects the bulk distribution coefficient or incompatibility of the elements in basaltic magma. Varying interpretations have resulted in a variety of elemental sequences (Sun et al., 1979; Pearce, 1982; Thompson et al., 1983; Hofmann et al., 1986; Sun and McDonough, 1989; Pearce and Parkinson, 1993), but the sequence is intended to produce systematic variations in incompatibility that result in smooth spidergram patterns for MORB; and consequently also for OIB. The spider diagram used here follows the elemental sequence of Sun and McDonough (1989), although K was exchanged with Nb and Ta to produce a smoother MORB pattern, and Cs and Pb have been omitted because many rocks lack these data. Sun and McDonough (1989) indicate that the order of elements U, Nb, Ta, and K is somewhat optional by indicating they have essentially equivalent incompatibilities. Figure 10 shows the resulting spidergrams for normal MORB (N-MORB), enriched MORB (E-MORB), OIB, and continental flood basalt (CFB), normalized to primitive mantle also as defined by Sun and McDonough (1989). These spidergrams stand in marked contrast to the irregular pattern produced by typical island-arc tholeiites and island-arc tholeiites-alkali basalt (IAT and IAT-AB) in Figure 11. The values used for typical IAT have been based on values by

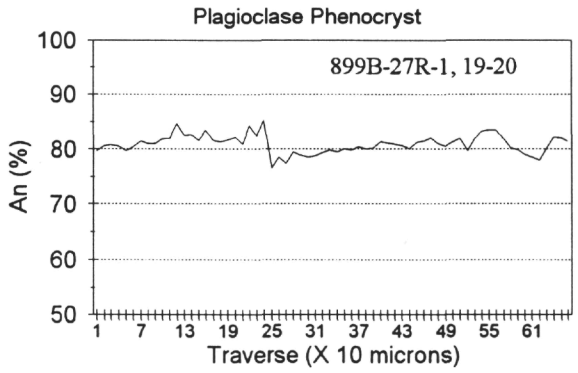

Figure 5. A microprobe traverse across a large plagioclase phenocryst in a basalt clast from interval 149-899B-27R-1, 19-26 cm, shows a lack of zoning and relatively constant composition near An_{80}.

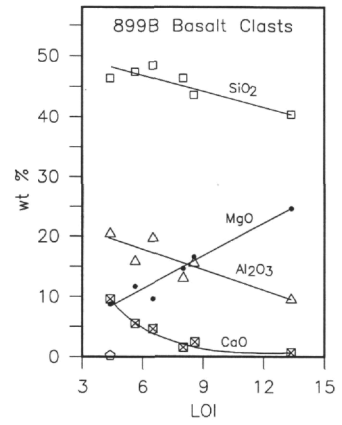

Figure 6. Several oxides in the basalt clasts vary systematically with variation in LOI content. SiO_2, $A1_2O_3$, and CaO decrease with increasing LOI, and MgO increases with increasing LOI.

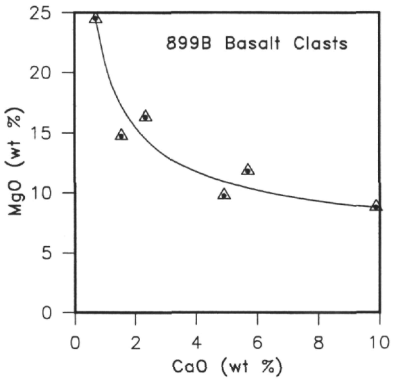

Figure 7. Highly modified MgO and CaO exhibit a strong negative correlation in the basalt clasts, suggesting that seafloor weathering effects are large relative to initial compositional variations.

Sun (1980) and other studies, with the range of compositions expressed by two spidergrams; one for IAT and another for IAT-AB.

A spidergram was derived for CFB, the most abundant type of continental basalt, to allow comparison with the various oceanic basalts. The resulting CFB spidergram represents an average of several flood basalts judged to be relatively free of contamination from continental lithosphere on the basis of published isotopic and trace element analyses (Bailey, 1989; Brannon, 1984; Dosso, 1984; Hooper

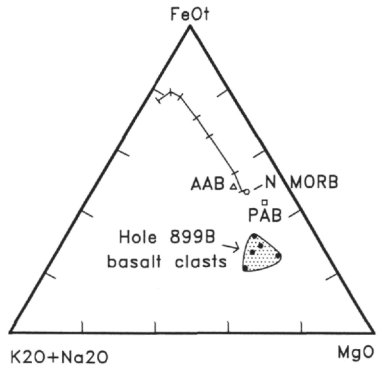

Figure 8. Basalt clasts plotted on an AFM diagram fall off the M (MgO) end of the Skaergaard magma evolution trend in a region typically characterized by cumulate rocks. Also plotted for comparison are a calculated primitive abyssal basalt (PAB) from Dick (1989), an average Atlantic abyssal basalt (AAB) from Melson et al. (1976), and an average N-MORB (N MORB) from Humphris et al. (1985).

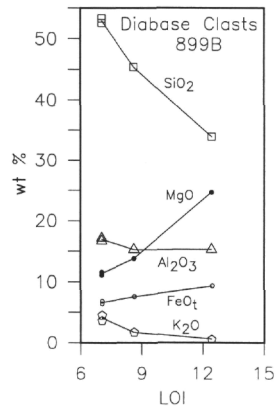

Figure 9. The oxides SiO_2, $A1_2O_3$, MgO, FeO_t, and K_2O vary systematically with variations in LOI content in the diabase clasts. Only MgO and FeO_t increase as LOI increases; the other oxides decrease.

and Hawkesworth, 1993; Lightfoot et al., 1993; Paces and Bell, 1989; Seifert et al., 1992; Wooden et al., 1993). The typical uncontaminated, or more likely slightly contaminated, CFB has a spidergram pattern rather similar to E-MORB, except for a Ba peak and a P low, with an elemental abundance between typical E-MORB and OIB (Fig. 10). The validity of the Ba peak and P low was checked by plotting individual flows used to derive typical CFB. They were found to have a wide variety of spidergrams that reflect the wide variability between individual CFB provinces. Continental basalts should be expected to be more variable than oceanic basalts because of their long path through highly variable continental lithosphere. Consequently, even if the two deviant elemental abundances on the typical CFB spidergram are real, and many individual flows have no significant peaks for these elements, the large variation among individual CFB flows limits their value as a distinctive test for a so-called typical CFB source. Furthermore, the similarity between spidergrams for E-MORB and the least contaminated CFB, ignoring the two deviant elements, makes distinction between these sources somewhat equivocal.

A total of six spidergrams has been derived for each basalt clast to allow visual comparison of the clast spidergram with primitive mantle (P-Mantle) and the typical basalt from each of the five major basalt provinces (Figs. 12-17). The overall similarity between IAT and IAT-AB allow comparison with either adequate for identification of an island-arc source province. A perfect match between a clast and a particular source is obtained when all of the elements on

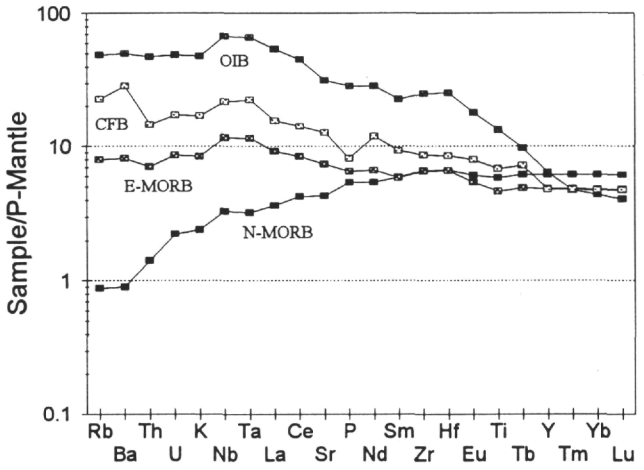

Figure 10. A spider diagram with spidergram patterns for N-MORB, E-MORB, OIB, and CFB using a slightly modified elemental sequence and normalizing values for P-Mantle from Sun and McDonough (1989). These spidergrams are relatively smooth except for the Ba peak and P low for CFB.

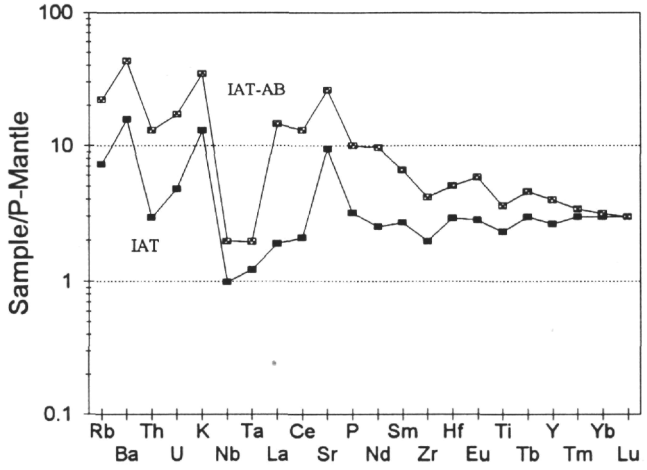

Figure 11. A spider diagram with spidergram patterns for IAT and IAT-AB using the same elemental sequence as Figure 10 and normalizing values from Sun (1980) and others. The irregular shape of the island-arc tholeiites stands in marked contrast to the relatively smooth patterns of the spidergrams in Figure 10.

the clast spidergram have a value of one. A perfect match would be interesting but no better than a relatively close match because the typical basalt for a given province probably does not actually exist. Comparison of clast spidergrams with the various basalt provinces shows that most basalt clasts exhibit a reasonable match with typical E-MORB or CFB, although the clast from interval 149-899B-27R-1, 19-26 cm (Fig. 12) plots between E-MORB and N-MORB. All clasts show anomalously high K peaks, and often high Rb, relative to that predicted for unaltered E-MORB or CFB. Spidergrams for clasts from interval 149-899B-26R-1, 113-118 cm (Fig. 13) and interval 149-899B-29R-1, 99-102 cm (Fig. 14) fall on the typical E-MORB and CFB abundance lines, whereas the clasts from interval 149-899B-27R-1, 13-15 cm (Fig. 15), interval 149-899B-27R-1, 33-40 cm (Fig. 16) and interval 149-899B-31R-1, 9-14 cm (Fig. 17) plot slightly above that line. Consequently, two samples are essentially equivalent to the typical E-MORB or CFB as plotted, whereas the three samples plotting slightly above the line are somewhat more enriched than typical E-MORB or CFB. Sample 149-899B-27R-1, 19-26 cm, is slightly more enriched than the typical N-MORB, crossing the equivalency line at a small angle, but falling below the abundance expected for E-MORB and CFB. All of the basalt clasts have distinctive Nb-Ta peaks relative to Nb-Ta depleted IAT, and consequently IAT-AB, indicating they are not derived from convergent plate boundaries.

Spider diagrams plot elements with varying characteristics and behavior and can be used to assess the relative mobility of the various elements if all elements have not been mobile. The REEs and high field-strength elements (HFSEs) are aligned on the basalt clast spidergrams and are typically regarded as the least mobile elements in aqueous solutions. High field strength elements on these spider diagrams include Hf, Zr, Ta, Nb, and Ti. Thorium can also behave in a similar manner. The remaining elements are mostly large ion lithophile elements (LILEs), which are notoriously mobile in aqueous solutions. LILEs plotted on these diagrams include K, Rb, Ba, and Sr. The LILEs commonly exhibit anomalous abundance peaks or lows on the basalt and diabase clast spidergrams relative to the less mobile REEs and HFSEs, confirming the mobility of LILEs during seafloor weathering. Uranium also commonly falls significantly off the immobile-element defined spidergram lines for these clasts, indicating it has also been mobile. Basalt clasts from interval 149-899B-27R-1, 19-26 cm (Fig. 15) and interval 149-899B-29R-1, 99-102 cm (Fig. 17) display above average amounts of Sr relative to typical E-MORB and CFB basalt province spidergrams, but less than the typical IAT spidergrams, that correlate with small positive Eu peaks contributed by the plagioclase phenocrysts in these clasts. Anomalous peaks for Sr and Eu are to be expected together in plagioclase phenocryst clasts because the ionic radii of these elements are very similar and both concentrate in the plagioclase lattice.

The REEs are regarded to be the least mobile elements during seafloor alteration processes (Ridley et al., 1994) and should best retain their primary igneous concentrations in these weathered basalt and diabase clasts. Despite the variable textures of the basalt clasts, all of the basalt clasts have smooth REE patterns similar to E-MORB, or less likely CFB, although the basalt clast with low TiO_2 and K_2O (interval 149-899B-27R-1,19-26 cm) has a flat transitional MORB, between E-MORB and N-MORB, REE pattern (Fig. 18). Both of the basalt clasts with plagioclase phenocrysts (interval 149-899B-27R-1, 19-26 cm, and interval 149-899B-29R-1, 99-102 cm) have the expected small positive Eu anomalies, although the anomaly is best developed in the clast from interval 149-899B-27R-1, 19-26 cm (Fig. 18). Despite the differences in textures, the REE patterns for all of the basalt clasts are similar, with a chondrite normalized abundance of the heavy rare earth elements (HREEs) near 10 times chondrite and the light rare earth elements (LREEs) with an abundance between 10 and 40 times chondrite. The similarity and smoothness of all REE patterns for the variably weathered basalt clasts indicates the REEs have not been significantly affected by seafloor weathering and all of the clasts have a transitional to enriched MORB origin or CFB origin. Obviously the spidergram patterns for E-MORB and least contaminated CFB are so similar that distinction between these basalt types is not easily possible with spidergrams. Isotopic data are needed to distinguish between E-MORB and least contaminated CFB.

The two diabase clasts (interval 149-899B-34R-1, 58-62 cm, and interval 149-899B-35R-1, 0-7 cm) analyzed for trace elements have spidergram and REE patterns similar to each other and to the most trace element depleted basalt clast (interval 149-899B-27R-1, 19-26 cm). The spidergrams for the two diabase clasts are similar, crossing the typical N-MORB line at a small angle and paralleling the E-MORB and CFB reference lines at slightly lower abundances (Figs. 19-20). Relative to MORB or CFB, and even the basalt clasts, the diabase clasts are more strongly enriched in K, Rb, and Ba, and slightly enriched in Sr. Elements K, Rb, and Ba were probably enriched during seafloor weathering and entered the secondary biotite observed in the diabase clasts. The enrichment of the diabase clasts in Nb-Ta indicates they are not convergent plate boundary Nb-Ta-depleted basalts. The REE patterns for the two diabase clasts are flat with an

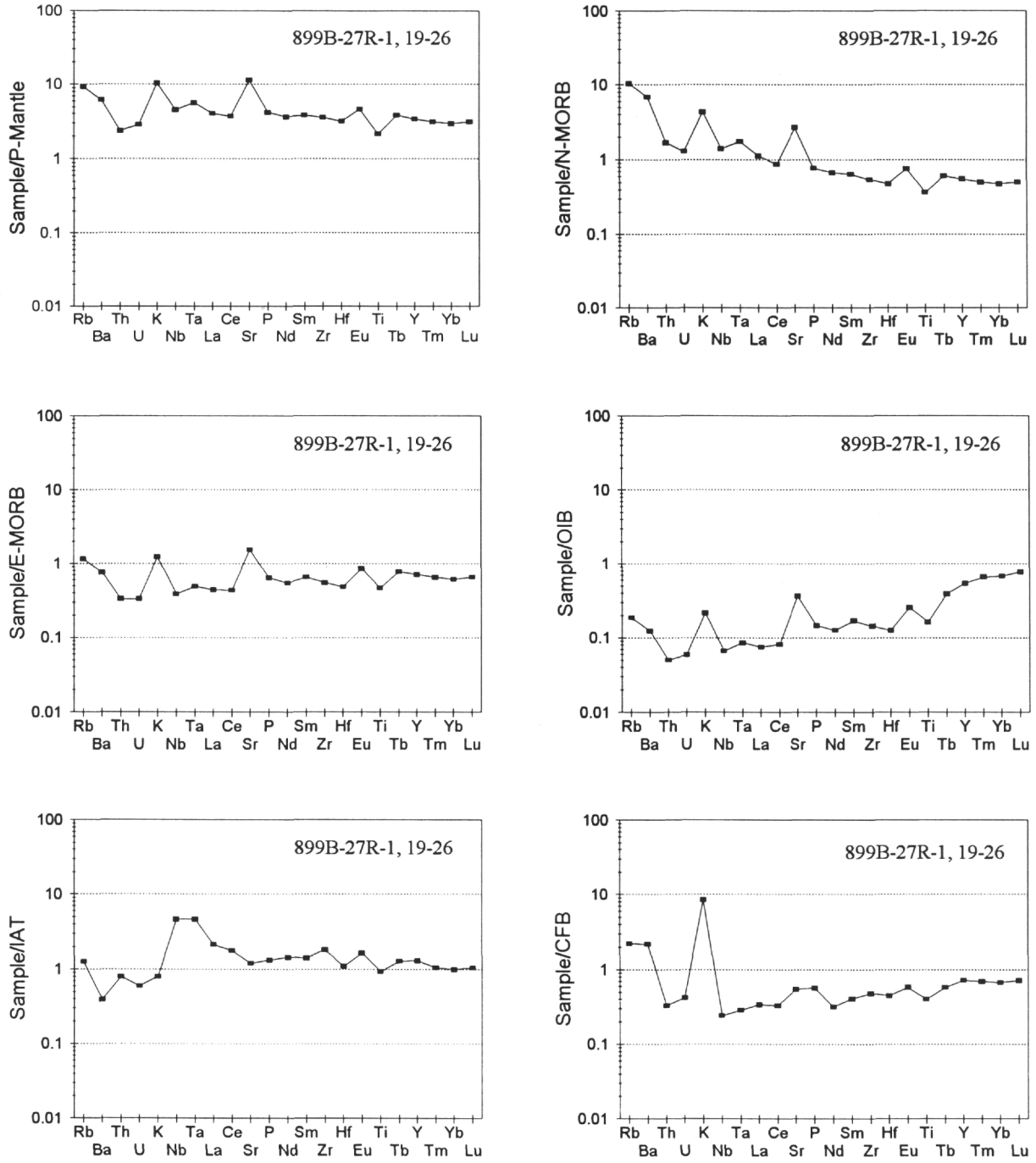

Figure 12. A spidergram for a basalt clast from interval 149-899B-27R-1, 19-26 cm, normalized to primitive mantle and the five common basalt provinces for comparison and source determination. This clast is slightly trace-element enriched relative to N-MORB and slightly depleted relative to E-MORB, which fits a transitional MORB source province. It contains unusually large Nb-Ta peaks relative to the typical Nb-Ta-depleted IAT spidergram. The enrichment in elements Rb, K, Sr, Eu, and Ba is unusually pronounced. Enrichment in Rb, Ba, and K is attributed to seafloor weathering, whereas enrichment in Sr and Eu is probably related to the plagioclase phenocrysts in this clast. Normalization values are from Sun (1989), Sun and McDonough (1989), and others as discussed in the text.

abundance near 10× chondrite and small positive Eu peaks (Fig. 21) indicating a transitional MORB or CFB origin.

DISCUSSION

The basalt and diabase clasts recovered from Hole 899B most closely resemble E-MORB similar to that characteristic of much of the present day Atlantic Ocean floor, or less likely CFB. The lack of CFB on the Iberia and Newfoundland continental margins adjacent to the Atlantic Ocean makes a CFB origin unlikely and would seem to indicate these clasts have a MORB origin. The extensive world wide MORB database has allowed detailed analysis of variations in the major element composition of clean MORB to search for compositional relationships and their causes (Klein and Langmuir, 1987; Brodholt and Batiza, 1989; Klein and Langmuir, 1989; Niu and Batiza, 1993). Even small-scale spatial and temporal variations of a local source are now being defined (Perfit et al., 1994). MORB compo-

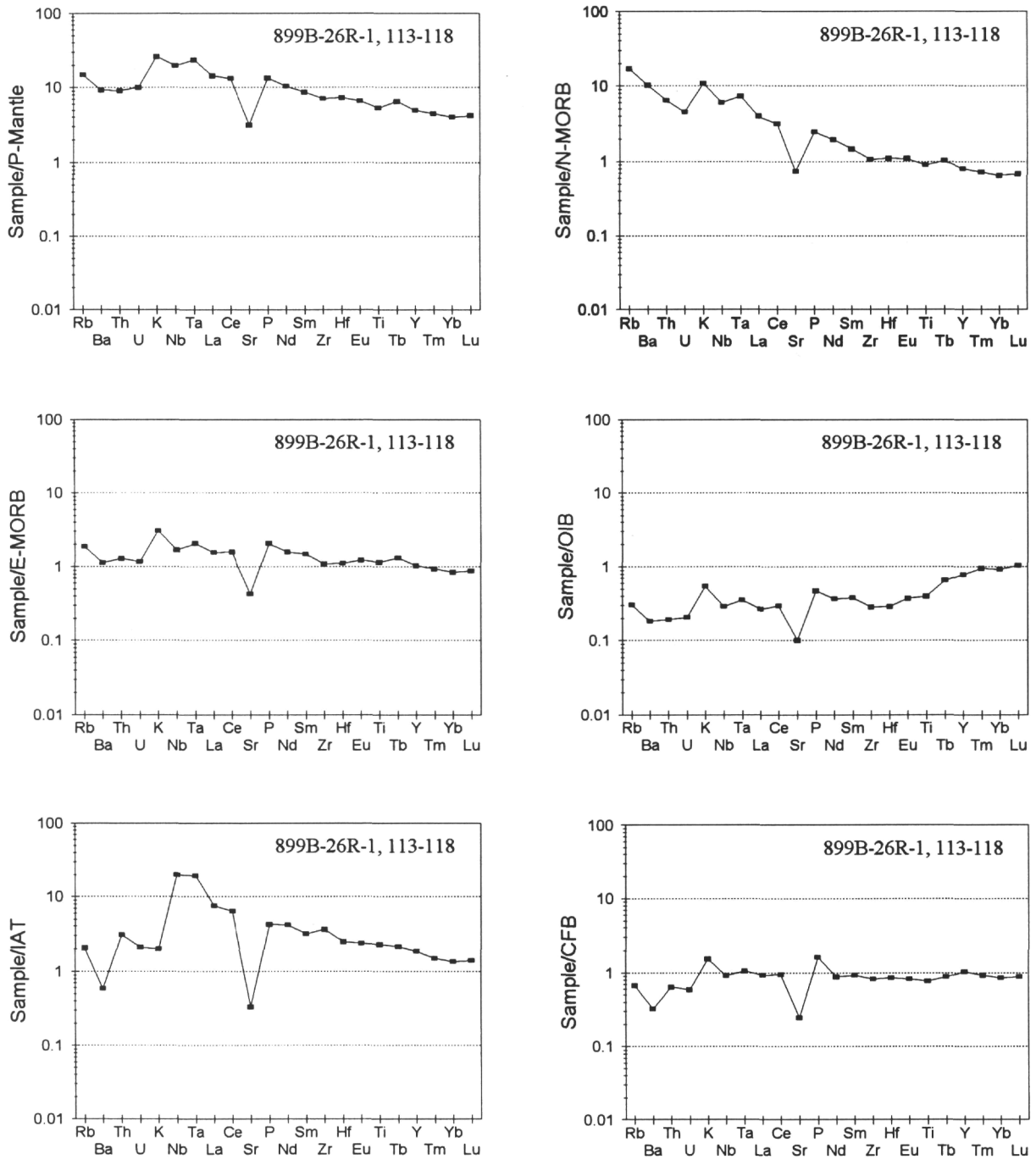

Figure 13. A spidergram for a basalt clast from interval 149-899B-26R-1, 113-118 cm, normalized to primitive mantle and the five common basalt provinces for comparison and source determination. Positive K and Rb peaks are attributed to addition of these elements during seafloor weathering, whereas the negative Sr peak is attributed to removal of Sr with Ca during seafloor weathering. The Ba low and the P peak relative to CFB may be caused by opposite peaks in the typical CFB spidergram (Fig. 10). Less mobile HREEs and HFSEs are parallel to E-MORB and CFB at a value of one, suggesting they are similar to basalts from these environments.

sitional data for the North Atlantic Ocean have been summarized by Bryan and Moore (1977), Langmuir et al. (1977); White and Bryan (1977); Bryan (1979); Bryan et al. (1981); Schilling et al. (1983); whereas Humphris et al. (1985) have provided compositional data for a portion of the southern Mid-Atlantic Ridge (MAR). The wide range in MORB composition along the length of the Mid-Atlantic Ridge and the enrichment of Azores Plateau basalts has been well illustrated by Schilling et al. (1983).

MAR basalt ranges from E-MORB at and near the plume generated Azores Plateau, including the FAMOUS area, to N-MORB from 49°N to 59°N to the north of the Azores Plateau and south of 33°N to the south of the Azores Plateau (Shibata et al., 1979). The E-MORB tholeiites that form the Azores Plateau are distinct from the incompatible element-rich alkali basalts that make up the Azores Islands themselves (White and Schilling, 1978; White et al., 1979). None of our clasts has either greatly enriched LREE patterns similar to the al-

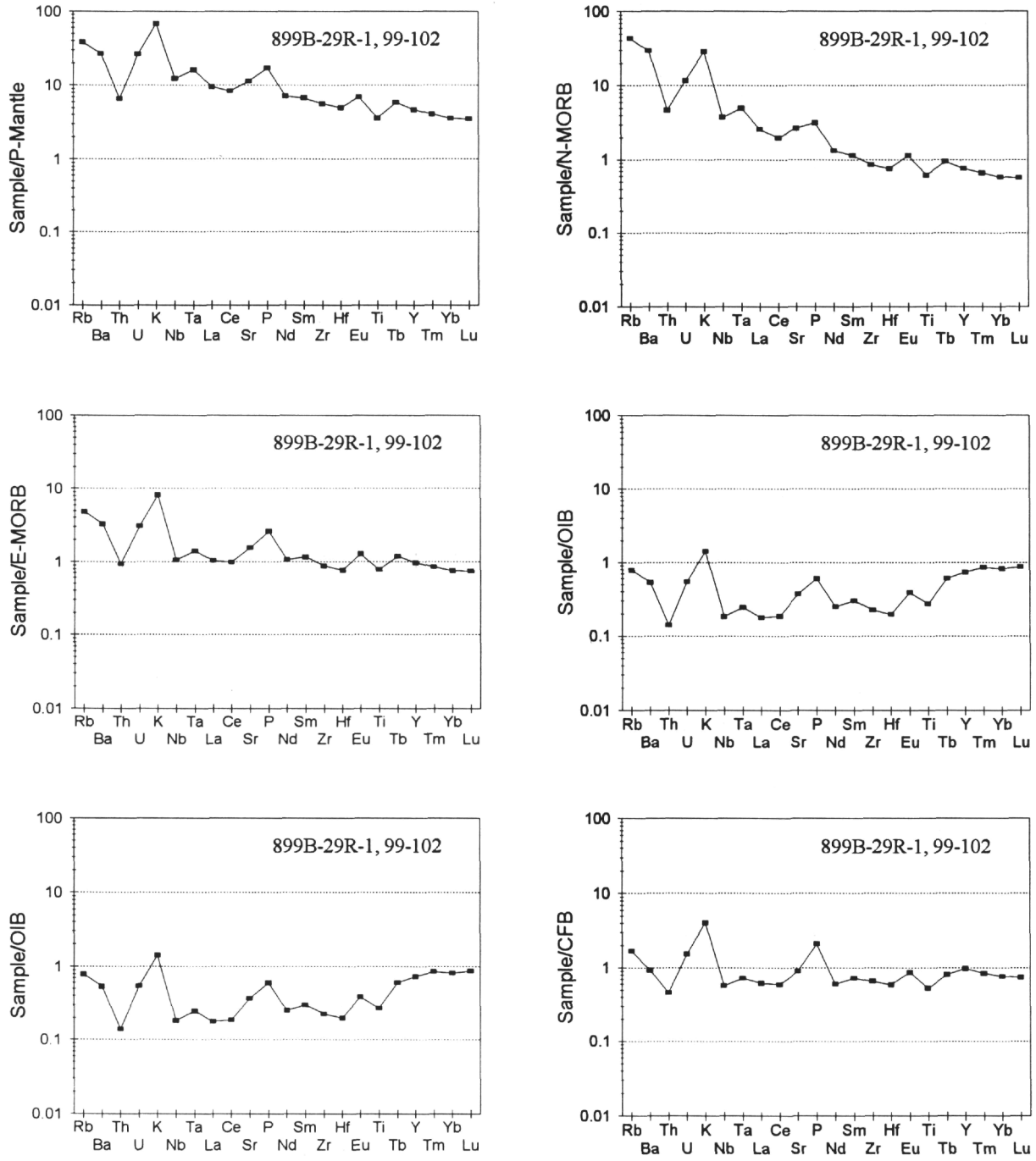

Figure 14. A spidergram for a basalt clast from interval 149-899B-29R-1, 99-102 cm, normalized to primitive mantle and the five common basalt provinces for comparison and source determination. The high Nb-Ta peak eliminates an IAT source, as it has for all the basalt clasts. Parallelism with the E-MORB and CFB again suggests that these provinces and the positive Sr and Eu peaks reflect the presence of the plagioclase phenocrysts in this clast. The typical Rb, K, Ba, and, to a lesser extent, U peaks appear to have been added by seafloor weathering. The reason for the P peak is not understood.

kali basalts of the Azores Islands (White et al., 1979) or depleted LREE patterns similar to nonplume-generated N-MORB that characterizes the regions north and south (Bryan et al., 1981) of the Azores Plateau region. All of the Hole 899B basalt and diabase clasts have incompatible element compositions similar to the much younger plume-generated E-MORB basalts from the nearby Azores Plateau (Schilling, 1975), with most basalt clasts resembling basalts from 37°-40°N. The one transitional basalt clast and diabase clasts more closely resemble the average FAMOUS basalt (Davies et al., 1989). Although plume-generated volcanism typically should be expected to result in abundant magmatism and the production of a volcanic rifted margin, the presence of a plume component is the only widely accepted mechanism to produce E-MORB. The presence of a plume component in basaltic rocks from this nonvolcanic rifted margin provides further evidence for multiple sources and magnitudes for plume components.

CONCLUSIONS

Both the texturally diverse basalt clasts and diabase clasts have similar and distinctive E-MORB immobile REE and HFSE incompatible element patterns. Much of the compositional variation among clasts resulted from seafloor weathering reactions that removed CaO and added LOI, MgO, and K_2O to the variably weathered clasts. The LILE have been variably affected by seafloor weathering reactions. The presence of E-MORB basalt and diabase clasts in Early Cretaceous sediments provides evidence for mantle plume-initiated rifting on the Iberia Abyssal Plain.

ACKNOWLEDGMENTS

The first author appreciates the opportunity to have been a shipboard petrologist on Leg 149, the guidance and co-operation of Co-Chief scientists Dale Sawyer and Bob Whitmarsh, and the support of an excellent technical staff and facilities on the ship. Data gathering for this study was supported by USSSP Grant# 0040 to the first author. This manuscript has been greatly improved by the constructive reviews of Bob Cullers and Bob Shuster as well as the comments of the ODP editorial staff.

REFERENCES

Anders, E., and Grevesse, N., 1989. Abundances of the elements: meteoritic and solar. *Geochim. Cosmochim. Acta,* 53:197—214.

Bailey, M.M., 1989. Evidence for magma recharge and assimilation in the Picture Gorge Basalt Subgroup, Columbia River Basalt Group. *In* Reidel, S.P., and Hooper, P.R. (Eds.), *Volcanism and Tectonism in the Columbia River Flood-Basalt Province.* Spec. Pap.—Geol. Soc. Am., 239:343-355.

Bischoff, J.L., and Dickson, F.W., 1975. Seawater-basalt interaction at 200°C and 500 bars: implications for origin of seafloor heavy metal deposits and regulation of seawater chemistry. *Earth Planet. Sci. Lett.,* 25:385-397.

Bischoff, J.L., and Seyfried, W.E., 1978. Hydrothermal chemistry of seawater from 25°C to 350°C. *Am. J. Sci,* 278:838-860.

Boillot, G., Winterer, E.L., Meyer, A.W., et al., 1987. *Proc. ODP, Init. Results,* 103: College Station, TX (Ocean Drilling Program).

Brannon, J.C., 1984. Geochemistry of successive lava flows of the Keweenawan North Shore Volcanic Group [Ph.D. dissert.]. Washington Univ., St. Louis, MO.

Brodholt, J.P., and Batiza, R., 1989. Global systematics of unaveraged mid-ocean ridge basalt compositions: comment on "Global correlations of ocean ridge basalt chemistry with axial depth and crustal thickness" by E.M. Klein and C.H. Langmuir. *J. Geophys. Res.,* 94:4231-4239.

Bryan, W.B., 1979. Regional variation and petrogenesis of basalt glasses from the FAMOUS area, Mid-Atlantic Ridge. *I. Petrol,* 20:293-325.

Bryan, W.B., and Moore, J.G., 1977. Compositional variations of young basalts in the Mid-Atlantic Ridge rift valley near lat 36°49'N. *Geol. Soc. Am. Bull.,* 88:556-570.

Bryan, W.B., Thompson, G., and Ludden, J.N., 1981. Compositional variation in normal MORB from 22°-25°N: Mid-Atlantic Ridge and Kane Fracture Zone. *J. Geophys. Res.,* 86:11815-11836.

Castillo, P.R., Carlson, R.W., and Batiza, R., 1991. Origin of Nauru Basin igneous complex: Sr, Nd, and Pb isotope and REE constraints. *Earth Planet. Sci. Lett.,* 103:200-213.

Davies, G.R., Norry, M.J., Gerlach, D.C., and Cliff, R.A., 1989. A combined chemical and Pb-Sr-Nd isotope study of the Azores and Cape Verde hotspots: the geodynamic implications. *In* Saunders, A.D., and Norry, M.J. (Eds.), *Magmatism in the Ocean Basins.* Geol. Soc. Spec. Publ. London, 42:231-255.

Dick, H.J.B., 1989. Abyssal peridotites, very slow spreading ridges and ocean ridge magmatism. *In* Saunders, A.D., and Norry, M.J. (Eds.), *Magmatism in the Ocean Basins.* Geol. Soc. Spec. Publ. London, 42:71-105.

Dosso, L., 1984. The nature of the Precambrian subcontinental mantle: isotopic study (strontium, lead, neodymium) of the Keweenawan volcanism of the north shore of Lake Superior [Ph.D. dissert.]. Univ. Minnesota, Minneapolis.

Floyd, P.A., 1989. Geochemical features of intraplate oceanic plateau basalts. *In* Saunders, A.D., and Norry, M.J. (Eds.), *Magmatism in the Ocean Basins.* Geol. Soc. Spec. Publ. London, 42:215-230.

Hajash, A., 1975. Hydrothermal processes along Mid-Ocean Ridges: an experimental investigation. *Contrib. Mineral. Petrol.,* 53:205-226.

Hajash, A., and Archer, P., 1980. Experimental seawater/basalt interactions: effects of cooling. *Contrib. Mineral. Petrol.,* 75:1-13.

Hofmann, A.W., Jochum, K.P., Seufert, M., and White, W.M., 1986. Nb and Pb in oceanic basalts: new constraints on mantle evolution. *Earth Planet. Sci. Lett.,* 79:33-45.

Hooper, P.R., and Hawkesworth, C.J., 1993. Isotopic and geochemical constraints on the origin and evolution of the Columbia River basalt. *J. Petrol,* 34:1202-1246.

Humphris, S.E., and Thompson, G., 1978. Hydrothermal alteration of oceanic basalts by seawater. *Geochim. Cosmochim. Acta,* 42:107-125.

Humphris, S.E., Thompson, G., Schilling, J.G., and Kingsley, R.H., 1985. Petrological and geochemical variations along the Mid-Atlantic Ridge between 46°S and 32°S: influence of the Tristan da Cunha mantle plume. *Geochim. Cosmochim. Acta,* 49:1445-1464.

Klein, E.M., and Langmuir, C.H., 1987. Global correlations of ocean ridge basalt chemistry with axial depth and crustal thickness. *J. Geophys. Res.,* 92:8089-8115.

———, 1989. Local versus global variations in ocean ridge basalt composition: a reply. *J. Geophys. Res.,* 94:4241-4252.

Langmuir, C.H., Bender, J.F., Bence, A.E., and Hanson, G.N., 1977. Petrogenesis of basalts from the FAMOUS area: Mid-Atlantic Ridge. *Earth Planet. Sci. Lett.,* 36:133-156.

Lightfoot, P.C., Hawkesworth, C.J., Hergt, J., Naldrett, A.J., Gorbachev, N.S., Fedorenko, V.A., and Doherty, W., 1993. Remobilisation of the continental lithosphere by a mantle plume: major-, trace-element, and Sr-, Nd-, and Pb-isotope evidence from picritic and tholeiitic lavas of the Noril'sk District, Siberian trap, Russia. *Contrib. Mineral Petrol,* 114:171-188.

Melson, W.G., Vallier, T.L., Wright, T.L., Byerly, G., and Nelen, J., 1976. Chemical diversity of abyssal volcanic glass erupted along Pacific, Atlantic, and Indian Ocean sea-floor spreading centers. *In* Sutton, G.H., Manghani, M.H., and Moberly, R. (Eds.), *The Geophysics of the Pacific Ocean Basin and Its Margin.* Geophys. Monogr., Am. Geophys. Union, 19:351-368.

Mottl, M.J., and Holland, H.D., 1978. Chemical exchange during hydrothermal alteration of basalt by seawater, I. Experimental results for major and minor components of seawater. *Geochim. Cosmochim. Acta,* 42:1103-1115.

Murillas, J., Mougenot, D., Boillot, G., Comas, M.C., Banda, E., and Maufret, A., 1990. Structure and evolution of the Galicia Interior basin (Atlantic western Iberian continental margin). *Tectonophysics,* 184:297-319.

Niu, Y., and Batiza, R., 1993. Chemical variation trends at fast and slow spreading mid-ocean ridges. *J. Geophys. Res.,* 98:7887-7902.

Paces, J.B., and Bell, K., 1989. Non-depleted sub-continental mantle beneath the Superior Province of the Canadian Shield: Nd-Sr isotopic and trace element evidence from Midcontinent Rift basalts. *Geochim. Cosmochim. Acta,* 53:2023-2035.

Pearce, J.A., 1982. Trace element characteristics of lavas from destructive plate boundaries. *In* Thorpe, R.S. (Ed.), *Andesites: Orogenic Andesites and Related Rocks:* New York (Wiley), 525-548.

Pearce, J.A., and Parkinson, I.J., 1993. Trace element models for mantle melting: application to volcanic arc petrogenesis. *In* Pritchard, H.M., Alabaster, T., Harris, N.B.W., and Neary, C.R. (Eds.), *Magmatic Processes and Plate Tectonics.* Geol. Soc. Spec. Publ. London, 76:373-403.

Perfit, M.R., Fornari, D.J., Smith, M.C., Bender, J.F., Langmuir, C.H., and Haymon, R.M., 1994. Small-scale spatial and temporal variations in mid-ocean ridge crest magmatic processes. *Geology,* 22:375-379.

Pinheiro, L.M., Whitmarsh, R.B., and Miles, P.R., 1992. The ocean-continent boundary off the western continental margin of Iberia, II. Crustal structure in the Tagus Abyssal Plain. *Geophys. J.,* 109:106-124.

Ridley, W.I., Perfit, M.R., Jonasson, I.R., and Smith, M.F., 1994. Hydrothermal alteration in oceanic ridge volcanics: a detailed study at the Galapagos fossil hydrothermal field. *Geochim. Cosmochim. Acta,* 58:2477-2494.

Sawyer, D.S., Whitmarsh, R.B., Klaus, A., et al., 1994. *Proc. ODP, Init. Repts.,* 149: College Station, TX (Ocean Drilling Program).

Schilling, J-G., 1975. Azores mantle blob: rare-earth evidence. *Earth Planet. Sci. Lett.,* 25:103-115.

Schilling, J.-G., Zajac, M, Evans, R., Johnston, T., White, W., Devine, J.D., and Kingsley, R., 1983. Petrologic and geochemical variations along the Mid-Atlantic ridge from 29°N to 73°N. *Am. J. Sci.,* 283:510-586.

Seifert, K.E., Peterman, Z.E., and Thieben, S.E., 1992. Possible crustal contamination of Midcontinent Rift igneous rocks: examples from the Mineral Lake intrusions, Wisconsin. *Can. J. Earth Sci.,* 29:1140-1153.

Seyfried, W.E., Jr., and Bischoff, J.L., 1979. Low temperature basalt-alteration by sea water: an experimental study at 70°C and 150°C. *Geochim. Cosmochim. Acta,* 43:1937-1948.

Shibata, T., Thompson, G., and Frey, F.A., 1979. Tholeiitic and alkali basalts from the Mid-Atlantic Ridge at 43°N. *Contrib. Mineral. Petrol,* 70:127-141.

Srivastava, S.P., Schouten, H., Roest, W.R., Klitgord, K.D., Kovacs, L.C., Verhoef, J., and Macnab, R., 1990. Iberian plate kinematics: a jumping plate boundary between Eurasia and Africa. *Nature,* 344:756-759.

Sun, S.-S., 1980. Lead isotopic study of young volcanic rocks from mid-ocean ridges, ocean islands and island arcs. *Philos. Trans. R. Soc. London A,* 297:409-445.

Sun, S.-S., and McDonough, W.F., 1989. Chemical and isotopic systematics of oceanic basalts: implications for mantle composition and processes. *In* Saunders, A.D., and Norry, M.J. (Eds.), *Magmatism in the Ocean Basins.* Geol. Soc. Spec. Publ. London, 42:313-345.

Sun, S.-S., Nesbitt, R.W., and Sharaskin, A.Y., 1979. Geochemical characteristics of mid-ocean ridge basalts. *Earth Planet. Sci. Lett.,* 44:119-138.

Thompson, G., 1973. A geochemical study of the low-temperature interaction of sea-water and oceanic igneous rocks. *Eos,* 54:1015-1019.

Thompson, G., and Humphris, S.E., 1977. Seawater-rock interactions in the oceanic basement. In *Proc.—Int. Symp. Water-Rock Interact., 2nd:* Strasbourg (IAGC), 13-18.

Thompson, R.N., Morrison, M.A., Dickin, A.P., and Hendry, G.L., 1983. Continental flood basalts...arachnids rule OK? *In* Hawkesworth, C.J., and Norry, M.J. (Eds.), *Continental Basalts and Mantle Xenoliths:* Cheshire, UK (Shiva), 158-185.

Vogt, P.R., and Perry, R.K., 1981. North Atlantic Ocean: bathymetry and plate tectonic evolution. *Geol. Soc. Am., Map and Chart Ser.,* MC-35.

White, W.M., and Bryan, W.B., 1977. Sr-isotope, K, Rb, Cs, Sr, Ba, and rare-earth geochemistry of basalts from the FAMOUS area. *Geol. Soc. Am. Bull.,* 88:571-576.

White, W.M., and Schilling, J-G., 1978. The nature and origin of geochemical variation in Mid-Atlantic Ridge basalts from the central north Atlantic. *Geochim. Cosmochim. Acta,* 42:1501-1516.

White, W.M., Tapia, M.D.M., and Schilling, J.-G., 1979. The petrology and geochemistry of the Azores Islands. *Contrib. Mineral. Petrol.,* 69:201-213.

Whitmarsh, R.B., Miles, P.R., and Mauffret, A., 1990. The ocean-continent boundary off the western continental margin of Iberia, I. Crustal structure at 40°30'N. *Geophys. J. Int.,* 103:509-531.

Wilson, R.C.L., Hiscott, R.N., Willis, M.G., and Gradstein, F.M., 1989. The Lusitanian Basin of west-central Portugal: Mesozoic and Tertiary tectonic, stratigraphic and subsidence history. *In* Tankard, A.J., and Balkwill, H.R. (Eds.), *Extensional Tectonics and Stratigraphy of the North Atlantic Margins.* AAPG Mem., 46:341-361.

Wooden, J.L., Czamanske, G.K., Fedorenko, V.A., Arndt, N.T., Chauvel, C., Bouse, R.M., King, B.W., Knight, R.J., and Siems, D.F., 1993. Isotopic and trace-element constraints on mantle and crustal contributions to Siberian continental flood basalts, Noril'sk area, Siberia. *Geochim. Cosmochim. Acta,* 57:3677-3704.

Date of initial receipt: 1 December 1994
Date of acceptance: 24 May 1995
Ms 149SR-225

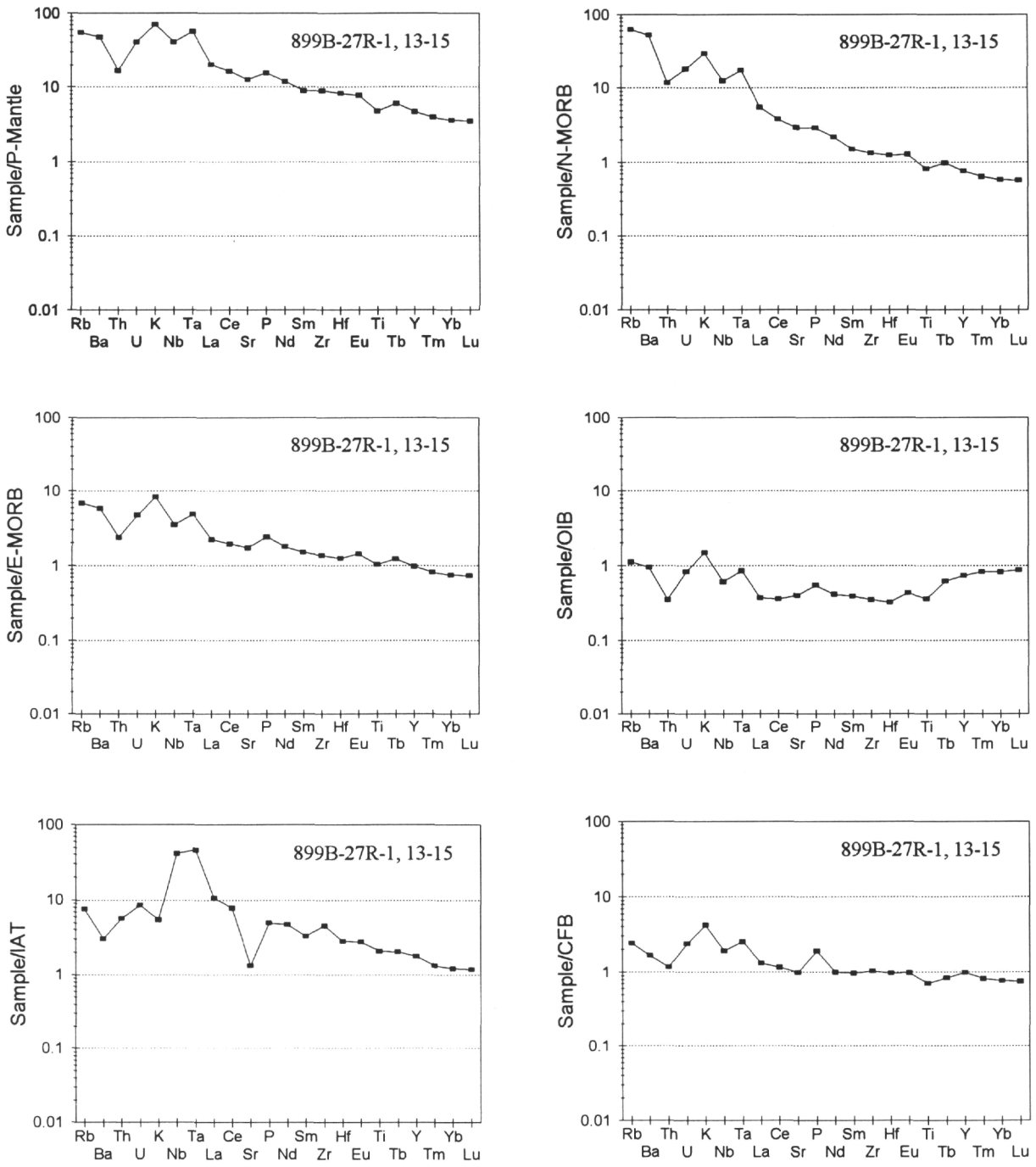

Figure 15. A spidergram for a basalt clast from interval 149-899B-27R-1, 13-15 cm, normalized to primitive mantle and the five common basalt provinces for comparison and source determination. The large Nb-Ta peaks relative to the IAT spidergram eliminate this environment as a possible source despite the parallelism of the less mobile elements at an abundance of one. This basalt clast is slightly more enriched in the LREE relative to HREE than either the typical E-MORB or CFB spidergrams, but are most similar to basalts from these environments. The negative Th peak relative to MORB and CFB spidergrams may indicate some removal by seafloor weathering. Ti values are also slightly low.

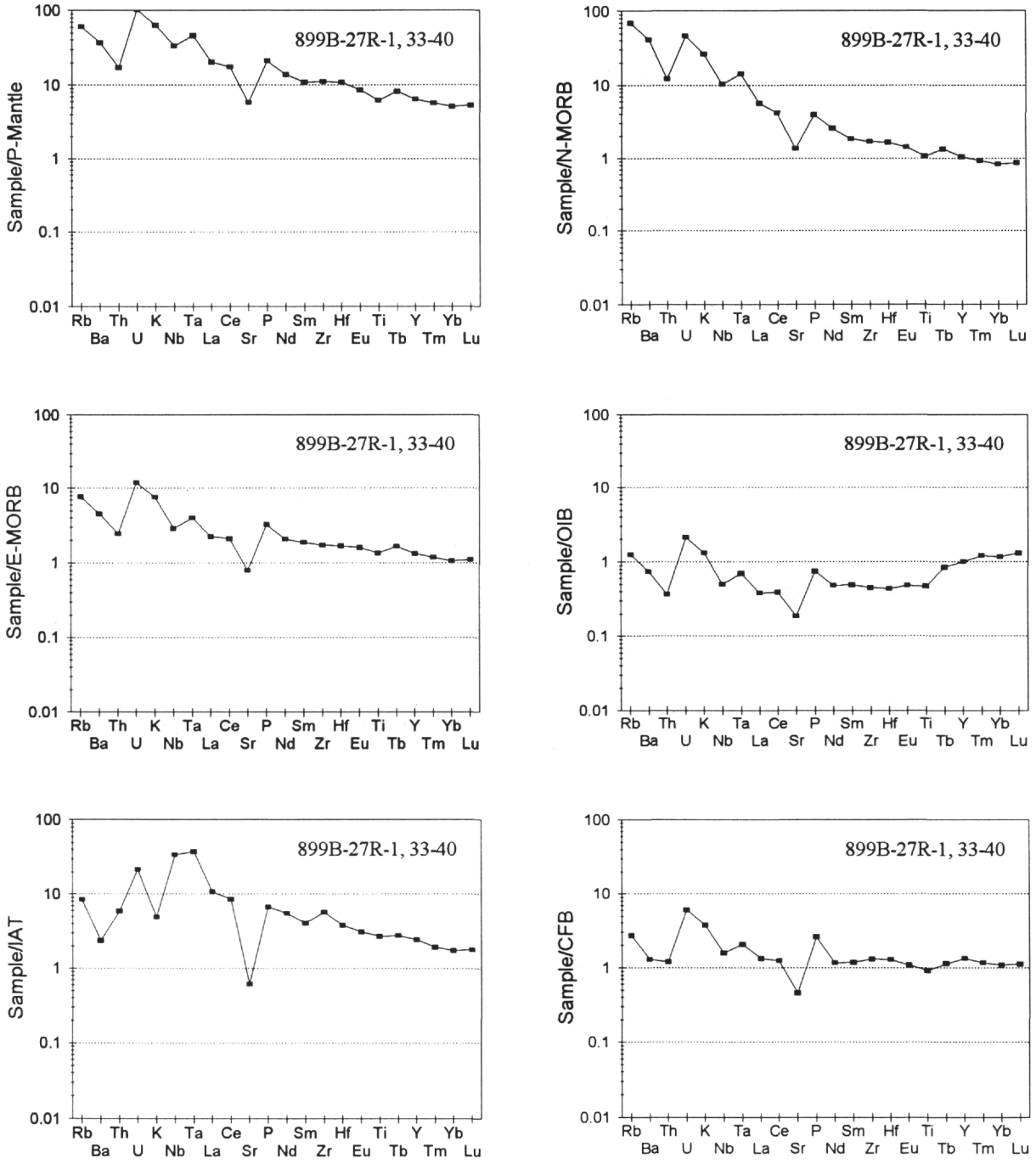

Figure 16. A spidergram for a basalt clast from interval 149-899B-27R-1, 33-40 cm, normalized to primitive mantle and the five common basalt provinces for comparison and source determination. This spidergram is not as parallel to the MORB spidergrams as the other basalt clasts, but the less mobile elements are similar in abundance to E-MORB, CFB, or even OIB. The high Nb-Ta values indicate it was not formed in an island-arc environment. The negative Sr peak probably relates to Ca removal during seafloor weathering. The positive U peak suggests it was added during seafloor weathering, and the addition of U and K accentuate an apparent negative Th peak that is actually rather small.

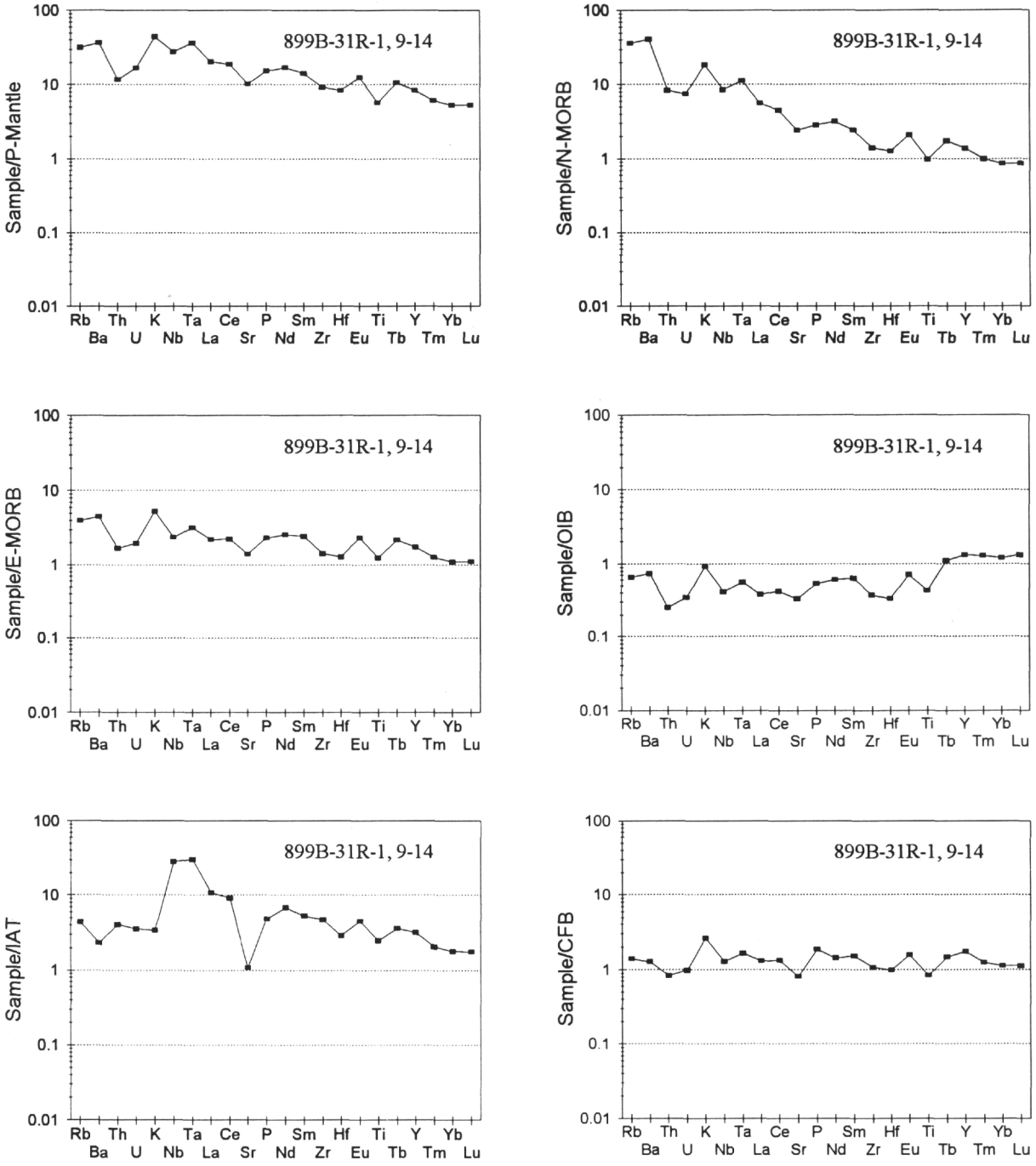

Figure 17. A spidergram for a basalt clast from interval 149-899B-31R-1, 9-14 cm, normalized to primitive mantle and the five common basalt provinces for comparison and source determination. The less mobile elements on this spidergram display a more irregular pattern than the other basalt clasts, with the HFSEs Zr, Hf, and Ti all having negative peaks. In addition, the usual seafloor weathering peaks are present with positive Rb and K peaks and a negative Sr peak. As usual, the strong Nb-Ta peak relative to the IAT spidergram indicates this clast is not from an island-arc.

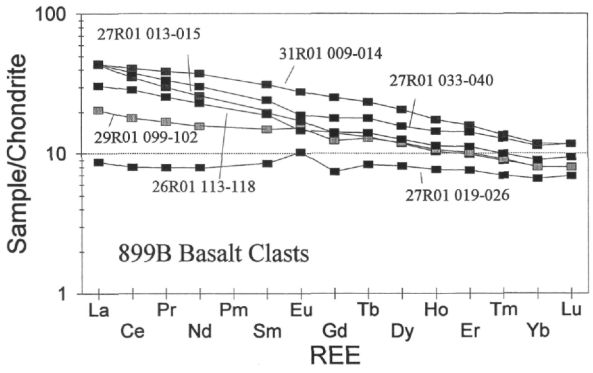

Figure 18. Chondrite-normalized REE patterns indicate all of the basalt clasts have enriched to transitional MORB origins with HREE abundances near 10× chondrite with little or no Eu anomalies. The chondrite values used for normalization are taken from Anders and Grevesse (1989) and multiplied by 1.36 to maintain consistency with older chondrite normalization values.

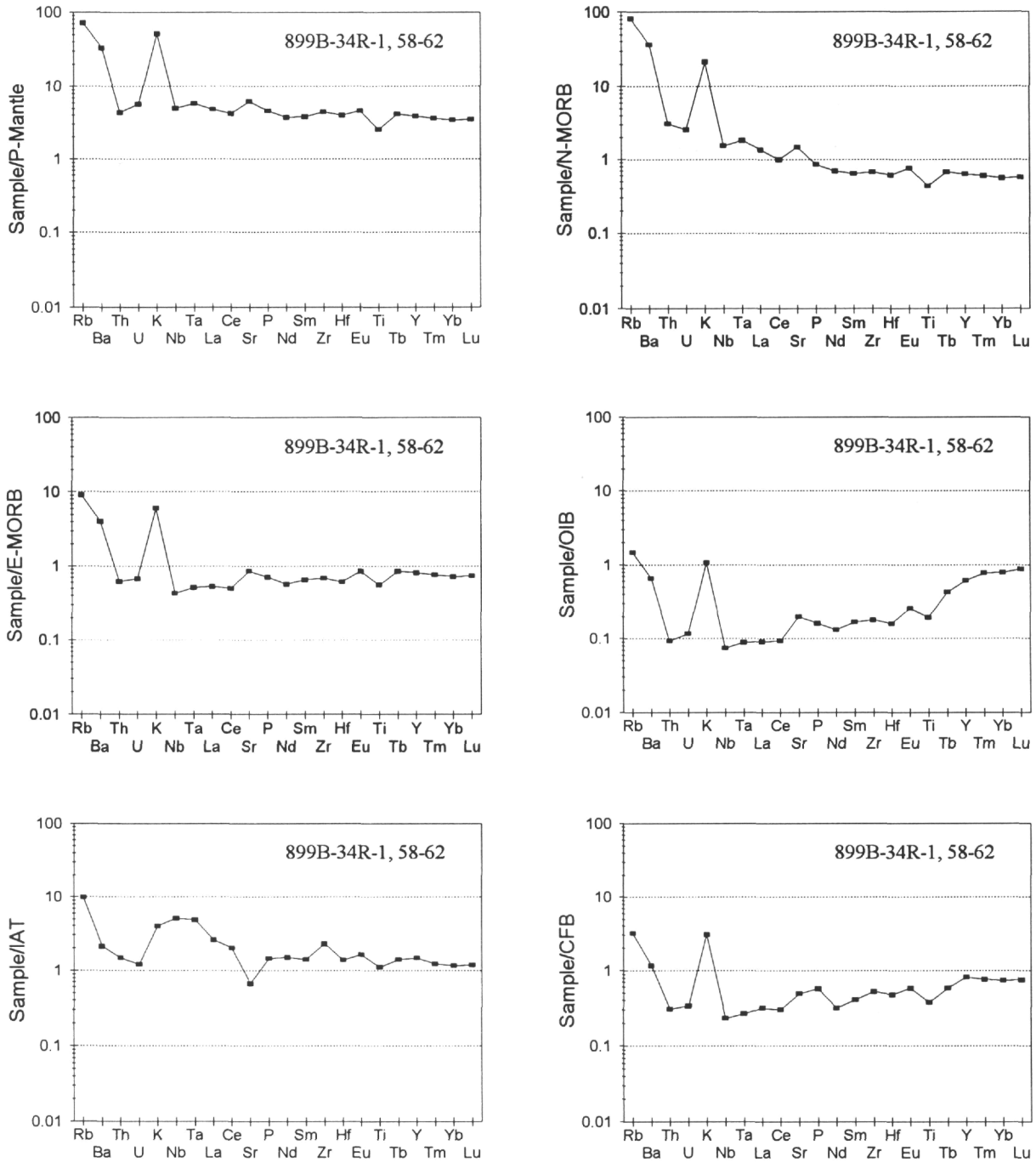

Figure 19. A spidergram for a diabase clast from interval 149-899B-34R-1, 58-62 cm, normalized to primitive mantle and the five common basalt provinces for comparison and source determination. The large Rb, Ba, and K peaks reflect the strong enrichment of these elements by seafloor weathering. These peaks are so large they obscure the typical strong Nb-Ta peak relative to the IAT spidergram, although it is still present. The positive Sr and Eu peaks must relate to the abundance of plagioclase in this clast.

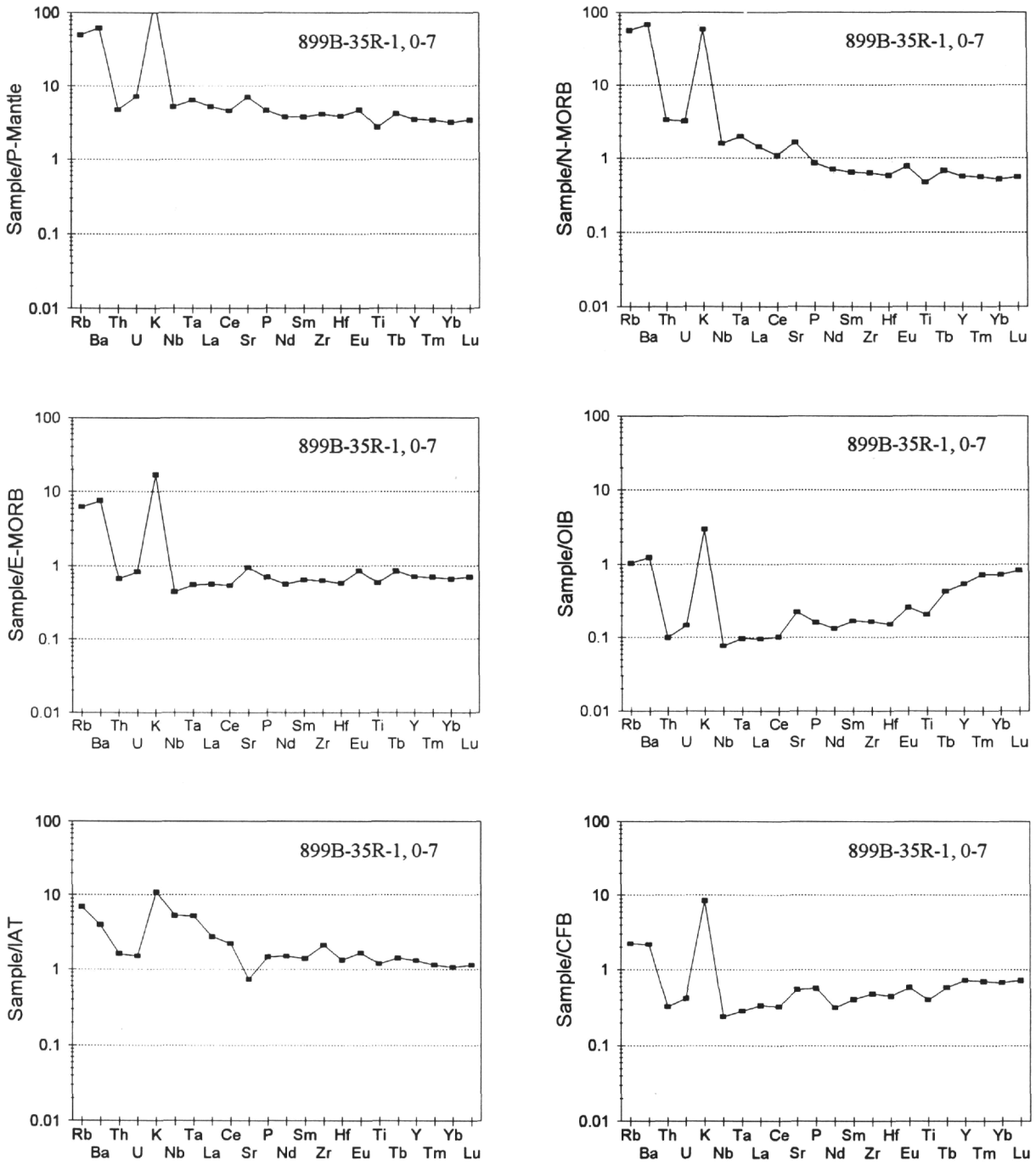

Figure 20. A spidergram for a diabase clast from interval 149-899B-35R-1, 0-7 cm, normalized to primitive mantle and the five common basalt provinces for comparison and source determination. The strong enrichment in Rb, Ba, and K by seafloor weathering is obvious in the large peaks for these elements. There are also small Sr and Eu peaks related to the abundance of plagioclase in this clast.

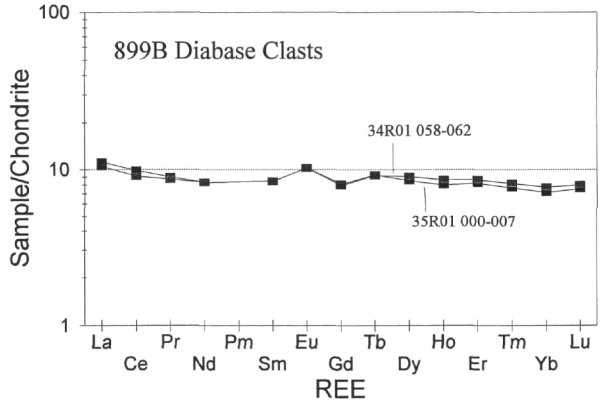

Figure 21. Chondrite normalized REE patterns for the two analyzed diabase clasts are nearly identical at 10× chondrite and indicate the clasts have a transitional MORB origin. Normalization values are the same as for Figure 18.